Atmospheric Environment 170 (2017) 197–204

Contents lists available at ScienceDirect

Atmospheric Environment

journal homepage: www.elsevier.com/locate/atmosenv

Influence of the West Pacific subtropical high on surface ozone daily variability in summertime over eastern China

Zijian Zhao [a], Yuxuan Wang [a, b, *]

[a] Department of Earth System Science, Tsinghua University, Beijing, China
[b] Department of Earth and Atmospheric Sciences, University of Houston, Houston, TX, United States

HIGHLIGHTS

- EOF analysis reveals the dominant component of ozone variability in eastern China is a marked north-south contrast.
- A stronger WPSH is associated with lower ozone in South China but with higher ozone in North China.
- This south-north difference can be explained by changing moisture transport associated with the WPSH variability.

ARTICLE INFO

Article history:
Received 20 May 2017
Received in revised form
4 September 2017
Accepted 16 September 2017
Available online 19 September 2017

Keywords:
West Pacific subtropical high
WPSH index
Surface ozone
Daily variations
Eastern China
Observations
Empirical orthogonal functions analysis

ABSTRACT

The West Pacific subtropical high (WPSH), as one of the most important components of the East Asian summer monsoon (EASM), is the key synoptic-scale circulation pattern influencing summertime precipitation and atmospheric conditions in China. Here we investigate the impacts of the WPSH on surface ozone daily variability over eastern China, using observations from recently established network of ozone monitors and meteorology reanalysis data during summer (June, July, August; JJA) 2014–2016 with a focus on 2014. An empirical orthogonal function (EOF) analysis of daily ozone variations reveals that the dominating eigenvector (EOF1), which contributes a quarter (25.2%) to the total variances, is a marked north-south contrast. This pattern is temporally well correlated ($r = -0.66$, $p < 0.01$) with daily anomalies of a normalized WPSH intensity index (WPSH-I). Spatially, the WPSH-I and ozone correlation is positive in North China (NC) but negative in South China (SC), which well correlates with the ozone EOF1 pattern showing the same north-south contrast ($r = -0.86$, $p < 0.01$). These associations suggest the dominant component of surface ozone daily variability in eastern China is linked with the variability of the WPSH intensity in that a stronger WPSH leads to a decrease of surface ozone over SC but an increase over NC and vice versa. This is because a stronger WPSH enhances southwesterly transport of moisture into SC, creating such conditions not conducive for ozone formation as higher RH, more cloudiness and precipitation, less UV radiation, and lower temperature. Meanwhile, as most of the rainfall due to the enhanced southwesterly transport of moisture occurs in SC, water vapor is largely depleted in the air masses transported towards NC, creating dry and sunny conditions over NC under a strong WPSH, thereby promoting ozone formation.

1. Introduction

Ozone is an important air pollutant and poses health and ecology problems on the ground level (Jacob and Winner, 2009; Kinney, 2008). Surface ozone concentrations depend on both emissions and meteorological conditions. Meteorological factors such as UV radiation, temperature, relative humidity (RH), and winds can influence ozone photochemical formation and dispersion processes (Bloomfield et al., 1996; Camalier et al., 2007; Leibensperger et al., 2008). High temperatures, typically associated with stagnant and sunny conditions, usually lead to high ozone events (Davis and Speckman, 1999; Steiner et al., 2010). As an indicator of atmospheric moisture, RH often shows a negative correlation with surface ozone (Elminir, 2005). Since the meteorological factors are not independent to each other but rather interconnected at certain spatiotemporal scales, the occurrence of high surface ozone

* Corresponding author. Department of Earth System Science, Tsinghua University, Beijing, China.
E-mail address: ywang246@central.uh.edu (Y. Wang).

https://doi.org/10.1016/j.atmosenv.2017.09.024
1352-2310/

concentrations cannot be attributed to one or few meteorological factors individually. For example, the synoptic-scale circulation patterns such as cold fronts, jet winds, and high-pressure systems have been identified as meteorological drivers affecting surface ozone variability (Chen et al., 2008; Shen et al., 2015; Zhu and Liang, 2013; Wang et al., 2016).

Previous studies have suggested that air quality over a large portion of East China in summer is subject to influences from the East Asian summer monsoon (EASM hereafter), and that these influences depend on the strength and tempo-spatial extension of the monsoon (Ding et al., 2013; Sun et al., 2016; Worden et al., 2009; Yamaji et al., 2006). On interannual scales, Yang et al. (2014) found a strong positive correlation between the EASM index and summer mean ozone over China during the period of 1986–2006 when the effects of changing anthropogenic emissions were removed. Wang et al. (2009) and Zhou et al. (2013) revealed that ozone enhancements in the free troposphere over coastal South China were associated with monsoon-induced transport of pollutants that originated from continental anthropogenic and biomass burning sources. At the surface, ozone exhibits a bi-modal seasonality in regions with strong EASM influences: monthly mean ozone peaks first in late spring (Apr or May), followed by a drop in the middle of summer (July and August) and the second peak in the fall (Sep or Oct). Such a summertime trough has been attributed to the influence of the EASM circulation (Li et al., 2007; Luo et al., 2000; Xu et al., 2008; Wang et al., 2008; Zheng et al., 2010). Through modeling analysis, Wang et al. (2011) suggested that the summer trough was resulted from a reduction in background ozone brought by the inflow of clean maritime air mass associated with the southeasterly monsoonal winds. While these studies clearly demonstrate the linkage of tropospheric ozone with the EASM on the interannual and seasonal scales, the extent to which the EASM impacts the daily ozone variability has yet to be characterized.

The West Pacific subtropical high (WPSH hereafter), as one of the most important components of the EASM, is the key synoptic pattern controlling daily weather conditions in east China during the monsoon season (Wang et al., 2006). The EASM begins to establish in late May and migrates to its most northern position by mid August. The northward migration of the EASM occurs in a stepwise fashion, characterized by two northward jumps of the WPSH and the related rain belt in mid-June and late-July (Su et al., 2014). This intraseasonal variability of the WPSH is related to the heat-induced unstable Rossby waves and the convective activities in the warm pool region (Chen et al., 1993; Lau and Peng, 2010; Su et al., 2014). The WPSH has thus been suggested as a key factor controlling the general areas of rain production in summer over east China (Gao et al., 2015; Liu et al., 2008). Liu et al. (2008) and Wang et al. (2006) demonstrated that the WPSH anomaly was responsible for the daily to sub-monthly regional weather anomalies linked with the extreme rainfall events over the Yangtze River Delta (YRD) region during the 1998 great flood in the Yangtze River basin. Since the position and intensity variations of the WPSH can change the regional temperature, precipitation, and wind conditions, they are expected to exert significant influences on ozone levels in east China. As a case study, He et al. (2012) found that ozone mixing ratios in a summer month at a surface site near Shanghai were often higher during the days when the center of the WPSH was located to the southeast of that site with a weaker intensity. Except for few cases, the daily-scale linkage of surface ozone with the WPSH variability in east China has not been systematically examined over the course of a summer season. In this study we will establish that such a linkage is significant on a daily scale, using ozone observations from the recently-established, extensive surface network in China. A mechanistic understanding of the factors responsible for the WPSH-ozone association will then be developed.

The rest of the paper is organized as follows. Section 2 describes the data source and methodology. Here daily variables of surface ozone and meteorological conditions during June, July, and August (JJA) are used to analyze the connection between the WPSH and ozone from 2014 to 2016, with a focus on 2014. Several indices for the WPSH are evaluated in order to characterize its variations. Section 3 summarizes summertime surface ozone distributions over east China and presents the spatial pattern of ozone daily variability using the empirical orthogonal functions (EOFs). Section 4 investigates the WPSH relationships with surface ozone on the daily scale. In Section 5, we analyze the mechanisms of the WPSH-ozone relationship. Section 6 discusses the drawbacks and potential implications.

2. Data and methodology

2.1. Ozone and meteorological observations

Hourly surface ozone concentrations were obtained from the China Ministry of Environment Protection (MEP, http://datacenter.mep.gov.cn/index). This data became available as an open dataset since 2013. The original unit of the MEP ozone observations is μg/m^3, which we converted to mixing ratios (unit: ppbv) using a constant temperature of 25 °C and pressure of 1013.25 hPa. There are 191 cities in China with ozone monitors in the dataset. If a city has more than one ozone monitors, they are averaged to represent mean ozone concentration of that city. Maximum daily 8-hour average (MDA8) ozone was calculated using hourly surface ozone mixing ratios. The following analysis uses MDA8 ozone of 191 cities in China during JJA (92 days) from 2014 to 2016, with a focus on 2014.

The meteorological data from 2014 to 2016 were obtained from the National Centers for Environmental Prediction (NCEP) Reanalysis dataset (Kalnay et al., 1996) and the European Center for Medium-Range Weather Forecasts (ECMWF) Reanalysis Interim (ERA-Interim) (Simmons et al., 2007). The NCEP and ERA-Interim Reanalysis data have a horizontal resolution of 2.5° × 2.5° and 0.5° × 0.5°, respectively, including mean daily geopotential height, meridional and zonal wind, RH, total cloud cover, downward UV radiation at the surface, 24-hour mean air temperature, and total precipitation amount per day.

2.2. WPSH index

Fig. 1 presents the climatological (1986–2005 mean) isolines and wind fields over the western Pacific in summer at 500 hPa. The

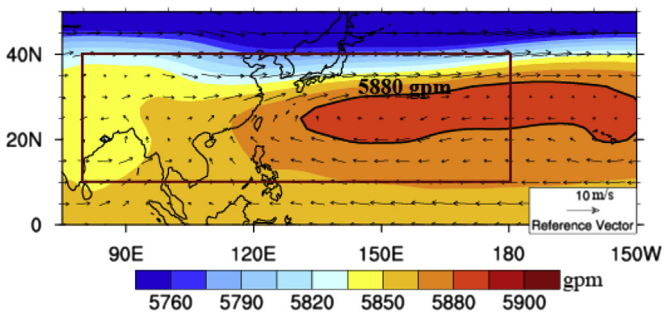

Fig. 1. The climatological position of the characteristic WPSH isoline and wind fields in summer at 500 hPa (measured by contour line for 5880 gpm). The red rectangle outlines the region used in the definition of WPSH-I. (For interpretation of the references to colour in this figure legend, the reader is referred to the web version of this article.)

WPSH is evident as a semi-permanent, sub-tropical anticyclone high pressure system extending from the surface to the middle troposphere over the western North Pacific (Tao and Xu, 1962; Zhou et al., 2009). As a deep high pressure system, the WPSH is conventionally described by circulation patterns at 500 hPa with a characteristic isoline of 5880 gpm (Ding, 1994; Wang et al., 2006). This isoline (Fig. 1) encircles a large region over the western Pacific (20°N −30°N, 130°E− 150°W). At the west side of the WPSH, 500 hPa winds change directions from southeasterly to southwesterly. Closer to the surface (not shown), the WPSH shifts more towards east and drives the low-level jet that transports a large amount of water vapor into East Asia (Lu, 2002).

In order to efficiently characterize the variability of the WPSH, we examined several WPSH indices from the literature that were used as metrics to describe its location and intensity. The WPSH intensity index (WPSH-I, defined below) was found to exhibit significant correlations with surface ozone in the YRD and were adopted for further analysis (Table S1). A number of other WPSH indices were used in the literature to depict the location of its ridge, western boundary, and northern boundary (Lu, 2002; Wang et al., 2006). No significant associations were found between those location-based indices and surface ozone (Table S1) and thus they are not discussed here. The WPSH-I is an indicator conventionally used and recommended by the National Climate Center in China (NCC) to represent the intensity of WPSH at a specified pressure level (500 hPa) (Lu, 2002; Wang et al., 2006). The definition domain of WPSH-I is chosen to be 10°N - 40°N and 80°E – 180°E (red rectangle in Fig. 1), which covers East Asia and the western Pacific, regions strongly influenced by the WPSH. The normalized WPSH-I index is calculated according to (1):

$$WPSH-I=\sum_{i=0}^{n}(H_i-H_0)\cdot\delta(H_i-H_0)/\mathrm{n} \quad (1)$$

Where δ is the function:

$$\delta(\mathrm{x})=\begin{cases}1, & \mathrm{x}>0\\ 0, & \mathrm{x}\le 0\end{cases} \quad (2)$$

where H_i is the geopotential height of a given grid i within the definition domain, n is the total number of the grids, and H_0 is the characteristic WPSH isoline of 5880 gpm at 500 hPa. According to (1), the WPSH-I index represents spatially accumulative enhancement of geopotential height above the WPSH characteristic isoline averaged over the definition domain. Daily mean 500 hPa geopotential height from the finer-resolution ERA dataset was used to calculate the WPSH-I index used in the subsequent analysis. For comparison, another set of the WPSH-I was calculated using the coarser-resolution NCEP reanalysis data. The two WPSH-I indices are highly correlated ($r = 0.98$) and have similar values (e.g. 2014 summer-mean WPSH-I of 0.68 from ERA and 0.79 from NCEP).

2.3. Data processing

Since the focus here is on daily variability, the MDA8 ozone and WPSH-I index were first de-seasonalized by subtracting 30-day moving averages from their original daily time series (Shen et al., 2015; Tai et al., 2010, 2012). The de-seasonalized time series of MDA8 ozone and WPSH-I show a significantly positive autocorrelation over a period of 3–7 days in eastern China (Figs. S1 and S2). To remove the compounding effects of such autocorrelation on daily variability, 5-day moving averages were applied for the de-seasonalized time series. We found these data processing procedures, while necessary, had only a slight effect on the ozone-WPSH relationships. Prior to data processing, the original time series of YRD-mean MDA8 ozone has a significantly negative correlation with the original WPSH-I time series (Fig. S3), with the Pearson correlation coefficient (r) of −0.45 ($p < 0.01$). This correlation changed to −0.33 ($p < 0.01$) and −0.70 ($p < 0.01$), respectively, when de-seasonalization and 5-day moving averages were applied to the original time series separately. When both de-seasonalization and 5-day moving averages were applied, the correlation became −0.50 ($p < 0.01$), only slightly different from that of the original time series. Unless stated otherwise, the ozone and WPSH-I anomalies hereafter are those daily residues after applying 5-day moving averages to the de-seasonalized time series.

2.4. EOF analysis

The empirical orthogonal function (EOF) analysis is a widely used multivariate statistical technique in atmospheric science to reveal both the spatial and temporal variations exhibited by the field being analyzed (Fiore et al., 2003; Shen et al., 2015; Pu et al., 2016; Wilks, 2011). The orthogonal functions composed by the EOF patterns are empirically defined to reconstruct the original field. Usually it is convenient to calculate the EOF patterns as linear combinations of the anomalies. Here the EOF analysis is applied to the daily MDA8 ozone anomalies at 191 Chinese cities during the 92 days in each summer season (JJA) from 2014 to 2016. For simplicity, we focus on the EOF results for the 2014 summer. Similar analysis of the 2015 and 2016 summer data is shown in the supplementary material.

3. Daily variations of summer surface ozone in the eastern China

3.1. Overview of ozone variability

Fig. 2a and b presents summer mean and standard deviations (SD) of MDA8 ozone at individual sites in 2014. Surface ozone is higher in eastern China because of higher precursor emissions. The SD is also the highest in east China, indicating larger influences by daily meteorological variations. Within eastern China, there is a clear south-to-north gradient in surface ozone mixing ratios. The seasonal mean MDA8 ozone is 67.37 ppbv over North China (NC, black rectangle in Fig. 2a), which is about 30% higher than that of 50.31 ppbv over South China (SC, red rectangle in Fig. 2a). The SD is similar between the two regions, at 15–20 ppbv.

Fig. 2c and d displays the mean and SD of MDA8 ozone during the three summers of 2014–2016. The spatial patterns are consistent to those in summer 2014, with a correlation coefficient r of 0.86 for the mean and 0.88 for the SD ($p < 0.01$) respectively. The 2014–2016 summer mean ozone have a south-to-north gradient of 14.90 ppbv (28.9%) between NC and SC, similar in magnitude to that in summer 2014. The average SD is similar between the two regions, at 17–18 ppbv, which is also similar in magnitude to that in summer 2014.

Comparing the available ozone observations during the three summers, summer 2014 was selected as a period of normal conditions on the basis of two considerations: first, the mean and SD of surface ozone in summer 2014 are similar and well correlated with that of the 2015 and 2016 (Fig. S4); second, the WPSH intensity during summer 2014 was similar to that of 2015 and 2016 (Fig. S5). The following analysis mainly uses ozone observations of 2014, focusing on the daily variability.

3.2. Ozone EOF patterns

Here the daily MDA8 ozone anomalies after data processing (described in Section 2.3) are used as the original field analyzed by

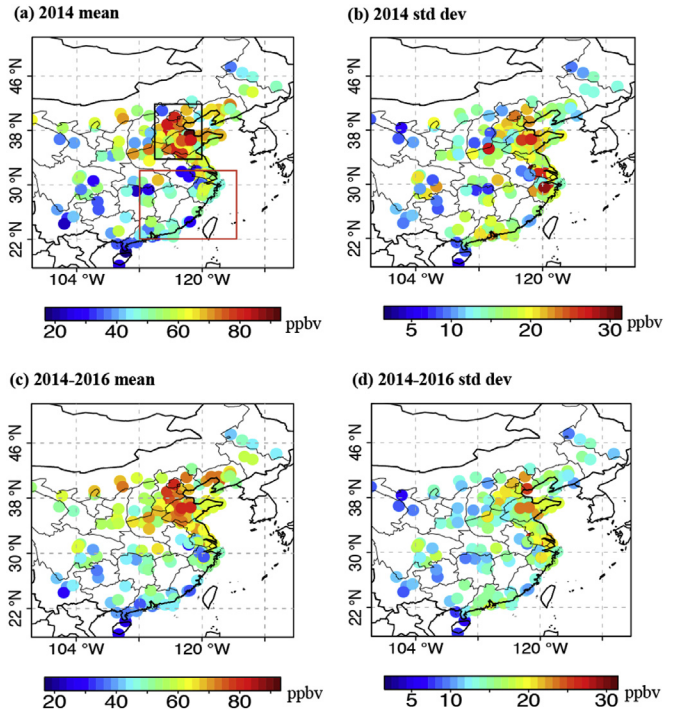

Fig. 2. Distribution of summer MDA8 ozone (a) mean and (b) standard deviation of 2014; Distribution of summer MDA8 ozone (c) mean and (d) standard deviation of 2014–2016. The black rectangle outlines North China (NC); the red rectangle outlines South China (SC). (For interpretation of the references to colour in this figure legend, the reader is referred to the web version of this article.)

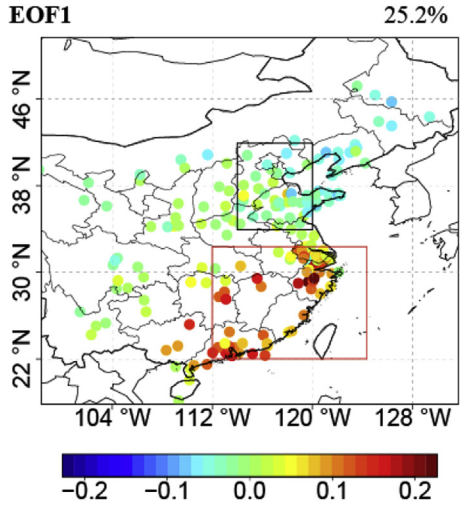

Fig. 3. The EOF1 of daily summer MDA8 ozone in 2014. The black rectangle outlines North China (NC); the red rectangle outlines South China (SC).

the EOF (described in Section 2.4) to reveal the spatial and temporal variations of surface ozone in east China. The first three EOF patterns of surface ozone in summer 2014 are shown in Fig. S6. Each EOF spatial pattern represents a share of the total variation of surface ozone that is proportional to its eigenvalue. Together the first three EOFs explain 49.4% of the variance in surface ozone, and the time series of each EOF pattern is uncorrelated with the time series of all the other EOF patterns. The first EOF pattern (EOF1) describes 25.2% of the total variance in daily MDA8 ozone concentrations. Interestingly, the EOF1 displays a north and south contrast (Fig. 3). The negative and positive values in the EOF patterns are expected to represent the extent of deviations from the normal surface ozone. The average of ozone variance in EOF1 is positive over SC (0.10) but negative over NC (−0.01). The EOF analysis was applied to the 2014–2016 summer mean daily MDA8 ozone distributions and the associated EOF1 pattern is similar to that of 2014 (Fig. S7). As the EOF1 pattern is commonly thought to represent the maximum possible fraction of the variability contained in the original data (Wilks, 2011) and in this case explains the most of surface ozone variability, the subsequent analysis focuses on the relationship of this pattern with WPSH.

4. WPSH relationship with ozone

We first examined the relationship between the WPSH intensity index and ozone on a daily scale. Fig. 4a shows the distribution of correlation coefficients between WSPH-I anomalies and MDA8 ozone anomalies in summer 2014. Correlation between WSPH-I and ozone is significantly negative in SC, and significantly positive in most parts of NC. The average correlation coefficient is −0.36 over SC ($p < 0.01$) and 0.20 ($p < 0.01$) over NC. The statistical significance of the correlations indicates that the daily variations of MDA8 ozone during summer may be linked with the WPSH-I variations. The different sign of the correlation coefficients between SC and NC indicates the north and south contrast in such relationship: a stronger WPSH intensity will lead to lower surface ozone in SC but higher ozone in NC. The spatial distribution of the correlation between WSPH-I and MDA8 ozone for the 2014–2016 summer mean conditions is consistent with that for summer 2014, showing significant correlations across eastern China and opposite signs of the correlation between SC and NC (Fig. S8).

The spatial distribution of the WPSH-ozone relationship shows an evident north and south contrast which appears to be similar to the EOF1 pattern of surface ozone displayed in Fig. 3. Indeed, the WPSH-ozone relationship is spatially well correlated with the ozone EOF1 pattern, with correlation coefficient (r) between the two at −0.86 ($p < 0.01$). In addition, as shown in Fig. 4b, the daily time series of ozone EOF1 and WPSH-I anomalies show a temporally significant correlation, with r of −0.66 ($p < 0.01$). Such spatial and temporal coherence suggests that the EOF1 pattern of surface ozone variations in China is linked with the WPSH-I variations. As the ozone EOF1 pattern has a negative correlation with WPSH-I, this indicates that a stronger WPSH intensity will lead to a decrease of surface ozone over SC but an increase over NC. The tight association between ozone EOF1 and WPSH-I suggests the dominant component of surface ozone daily variability in eastern China is linked with the variability in the WPSH intensity.

To test the robustness of the relationship between surface ozone and the WPSH-I index using the ERA reanalysis, we conducted the same analysis using WPSH-I derived from the NCEP reanalysis (Fig. 4b). The time series of NCEP WPSH-I and ERA WPSH-I during summer 2014 are significantly correlated with r of 0.98 ($p < 0.01$). Spatially, the distribution of correlation coefficients between NCEP WPSH-I anomalies and MDA8 ozone anomalies are well correlated ($r = 0.99$, $p < 0.01$), consistent with the spatial pattern shown in Fig. 4a using the ERA WPSH-I (Fig. S9). Significant negative and positive correlations are consistently found between the NCEP WPSH-I and surface ozone over SC and NC, respectively. In addition, the daily time series of ozone EOF1 and NCEP WPSH-I anomalies are significantly correlated ($r = -0.67$, $p < 0.01$). The consistency between the two WPSH-I indices indicates the robustness of the WPSH-I indicator developed here with regards to its ability of explaining the daily variability of surface ozone over eastern China.

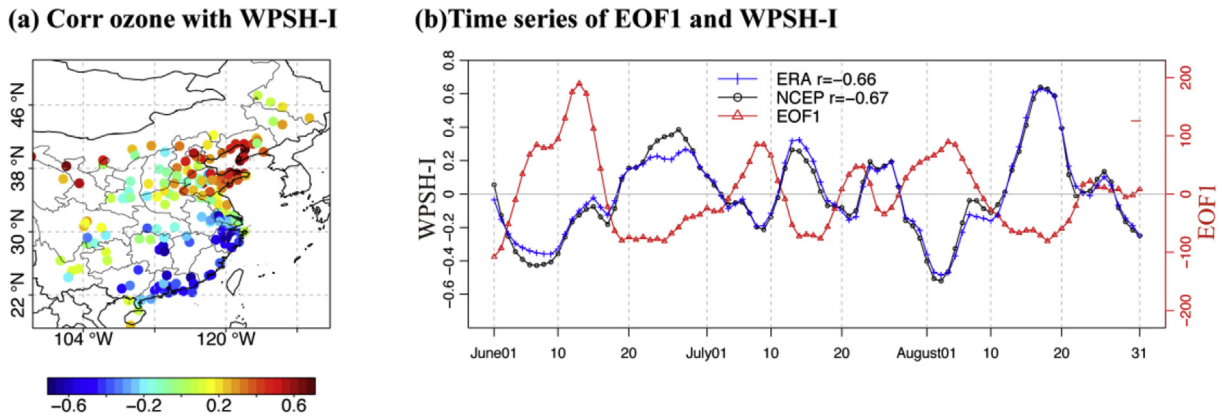

Fig. 4. (a) Correlation coefficients between surface ozone and WPSH-I, and (b) the time series of the first EOF loading (red line, right y-axis) and the WPSH-I (blue line for ERA WPSH-I and black line for NCEP WPSH-I, left y-axis) during the summer of 2014. The correlation coefficient between WPSH-I and ozone is shown in (b).

5. Mechanism

We discuss in this section the mechanisms underlying the observed association between WPSH intensity and summertime ozone daily variations over eastern China presented above. Firstly, the influence of WPSH-I variations on circulation patterns is investigated, focusing on the horizontal wind fields from the surface to the lower troposphere. Secondly, we examine how such changes in wind fields affect the moisture transport and precipitation. Finally, we analyze the north-south contrast in atmospheric conditions of importance to surface ozone - including cloudiness, UV radiation, and temperature - and the linkage of such contrast to WPSH-I variability.

Previous studies suggested that precipitation along the Yangtze River (in SC) had a significant positive correlation with the intensity of the WPSH, whereas summer rainfall in North China had a negative correlation with the WPSH (Gao et al., 2015; Liu et al., 2008). Such patterns indicate that the WPSH variability can lead to changes of moisture transport. To illustrate the variations of moisture advection due to WPSH, Fig. 5a displays the distribution of 850 hPa wind fields during summer 2014. Here the 850 hPa level is chosen as an approximation of the lower troposphere conditions of importance for surface ozone. As EASM drives maritime air masses marching inland, there is a decreasing trend of wind speeds from south to north and east to west. The southwesterly winds larger than 5 m/s are found over the coastal SC, indicating the strongest influence of the WPSH and EASM there. The summer mean wind speed is lower in NC than in SC. To understand the changes of wind speed due to WPSH-I variations, the summer days were divided into low and high WPSH-I days using the daily WPSH-I anomalies: high WPSH-I days are those with positive WPSH-I anomalies and low WPSH-I days have negative WPSH-I anomalies. Table 1 summarizes summertime mean zonal (U) and meridional (V) wind speeds over SC and NC at different vertical levels (10 m above the surface and 850 hPa) for the averages of all summer days, and low and high WPSH-I days. In the low WPSH-I days, both U and V wind component over SC are lower at near-surface and 850 hPa. In the high WPSH-I days, compared with the summer mean, both U and V wind over SC are increased by 71%–109% at both near-surface and 850 hPa levels. In NC, however, the changes of U and V wind speeds during the low and high WPSH-I days are not obvious. Fig. 5d shows the correlation coefficient, r, between the daily WPSH-I anomaly and 850 hPa wind speed, overlaid with the 850 hPa wind anomalies during the high WPSH-I days shown as vector. The spatial distribution of r reveals a strong positive correlation of WPSH-I and the 850 hPa wind speed on SC, with the greatest correlation centered in a swath extending over the Southeast China at 850 hPa. The wind anomalies are associated with the strongest correlations of WPSH-I and wind speeds, indicating strong winds coming from the South China Sea. Such pattern of wind anomalies is obvious not only at 850 hPa but also at 10 m (Fig. S10), indicative of the stronger southwesterly extending from the lower troposphere to the surface. However, the WPSH-I variations show less significant correlations with wind speeds in NC, suggesting that the changes of WPSH intensity exert less influence on circulation patterns over NC.

Fig. 5b–c shows the distribution of near-surface (2 m from the surface) RH and daily precipitation during summer 2014, depicting significantly higher RH and rainfall over SC (>70% and >7 mm/day) than that over NC (<70% and < 3 mm/day) that is consistent with the south-to-north transport of moisture shown in Fig. 5a. As a stronger WPSH intensity results in stronger southwesterly over SC (c.f. Fig. 5d), the enhanced southwesterly transports more water vapor and warm air mass from South China Sea, which in turn lead to more precipitation in SC when intersecting with continental air from the north. Indeed, Fig. 5e–f shows the strong positive correlation of daily RH and total precipitation in SC with WPSH-I, confirming the more abundant water vapor conditions and rainfall associated with stronger WPSH intensity for this region.

Uplift and moisture supply are two indispensable factors for precipitation to occur. As most of the rainfall associated with the enhanced southwesterly transport of moisture occurs in SC, water vapor is thus highly reduced in the air masses transported towards NC. Indeed, the RH and precipitation over NC both show a negative correlation with WPSH-I, suggesting a reduction of moisture transport into that region under stronger WPSH intensity conditions. The average RH over NC is lower than 70% during the high WPSH-I days (Table 1), poor moisture conditions not conducive for synoptic-scale cloud development and precipitation. Table 1 also compares the regional-mean daily precipitation between the low and high WPSH-I days over both NC and SC, showing the north-to-source differences consistent with the correlation patterns in Fig. 5f.

While ozone is only slightly soluble and thus not efficiently scavenged by precipitation, precipitation is usually accompanied with more cloudiness, less UV radiation, and lower temperature, conditions not conducive for photochemical production of ozone. Fig. 6a–c presents the distribution of total cloud cover (TCC), downward UV radiation at the surface, and near-surface (2 m from the surface) temperature during summer 2014, respectively. Corresponding to the spatial pattern of the moisture-related fields in

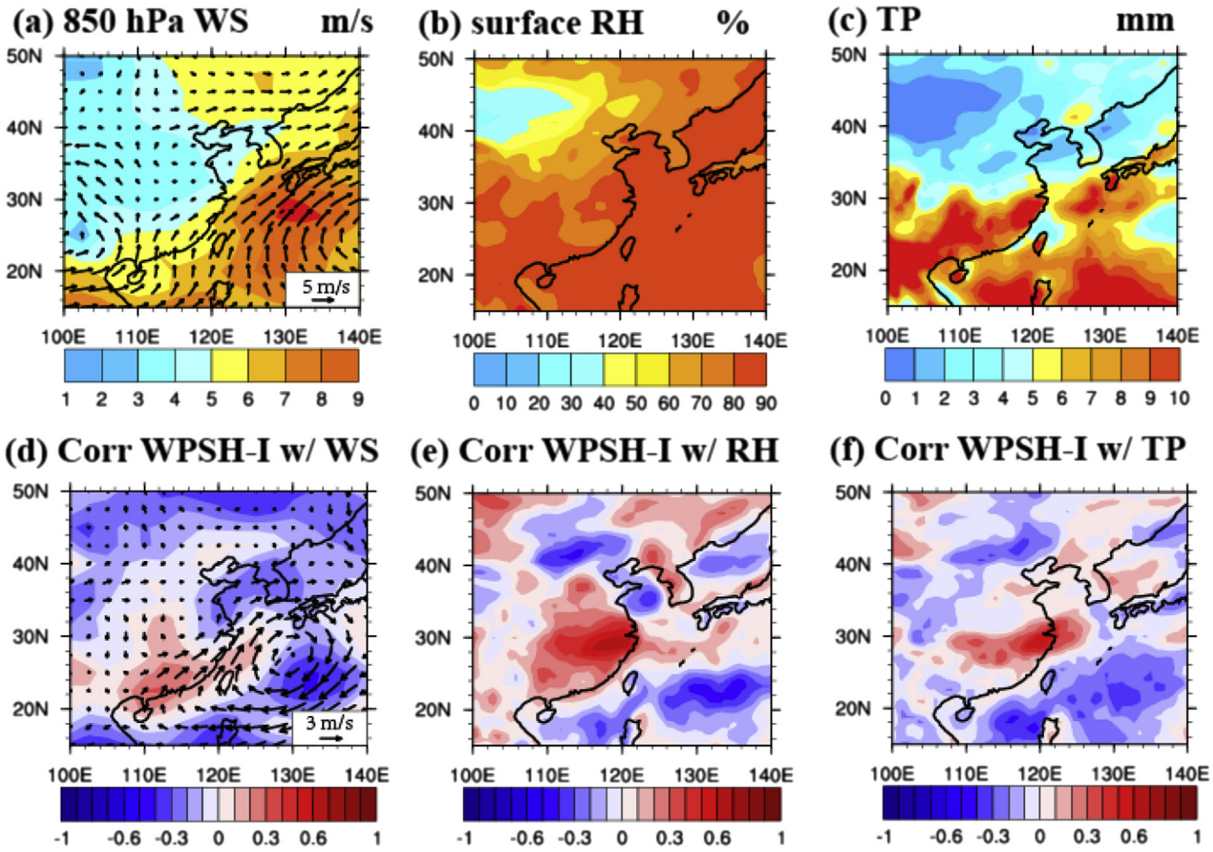

Fig. 5. (Upper panel) the summer mean fields of meteorological parameters and (lower panel) their correlations with the daily WPSH-I anomalies: 850 hPa wind speed (a, d), near-surface RH (b, e), and daily total precipitation (c, f). The 850 hPa wind fields are shown as black arrows in (a) and wind anomalies as black arrows in (d).

Fig. 5, SC has a higher TCC, lower UV radiation, and higher temperature than NC in summer (Table 1). With regards to the day-to-day variability, there is a strong positive correlation of TCC with WPSH-I in SC, indicating higher TCC linked with stronger WPSH, while no correlation between the two is found in NC (Fig. 6d). Correspondingly, the correlation of WPSH-I with both the UV radiation and temperature is negative in SC and positive in NC (Fig. 6e–f). Compared with the low WPSH-I days, the high WPSH-I days over SC saw a 17% increase of TCC, a 14% decrease of UV radiation at surface and a 0.73 and 0.59 K decrease of temperature at 850 hPa and near-surface. The corresponding changes of over NC are all opposite in sign and smaller in magnitude (Table 1). Particularly, NC experiences stronger UV radiation during the high WPSH-I days, indicative of more suitable atmospheric conditions conducive for high ozone.

In summary, a stronger WPSH intensity is associated with stronger southwesterly winds at the western edge of the WPSH which transport more moisture from the South China Sea into SC. This brings atmospheric conditions of higher RH and more rainfall, accompanying with more cloudiness, less UV radiation, and lower temperatures over SC. However, the changes of southwesterly winds due to WPSH intensity variation do not extend to NC. On the contrary, as water vapor is highly reduced in the air masses transported towards NC, a stronger WPSH intensity will bring the typical high pressure conditions over NC with drier atmospheric conditions featuring lower RH, less cloudiness, and more UV

Table 1
The average of meridional wind (V), zonal wind (U), relative humidity (RH), air temperature (T) at different vertical levels and daily total precipitation (TP), total cloud cover (TCC), and downward UV radiation at the surface (UV) over South China and North China during the whole summer, high WPSH-I days and low WPSH-I days in 2014.

Parameter	Level	SC			NC		
		High WPSH-I days	Low WPSH-I days	Summer mean	High WPSH-I days	Low WPSH-I days	Summer mean
V (m/s)	10 m	1.59	0.14	0.8	0.65	0.5	0.57
	850 hPa	2.32	0.55	1.36	0.55	0.43	0.47
U (m/s)	10 m	−0.09	−0.46	−0.29	0.25	0.15	0.2
	850 hPa	1.63	0.06	0.78	0.98	0.82	0.89
RH (%)	2 m	84.11	80.25	82.01	62.8	63.85	63.37
	850 hPa	74.86	70.1	72.28	51.86	58.12	55.26
T (K)	2 m	300.08	300.67	300.4	296.62	296.89	296.77
	850 hPa	292.74	293.47	293.14	291.63	291.42	291.51
TP (mm)	/	8.22	6.07	7.05	2.34	2.43	2.39
TCC	/	0.74	0.63	0.68	0.47	0.54	0.51
UV (kJ/m^2)	/	75.78	87.73	82.27	91.4	89.95	90.61

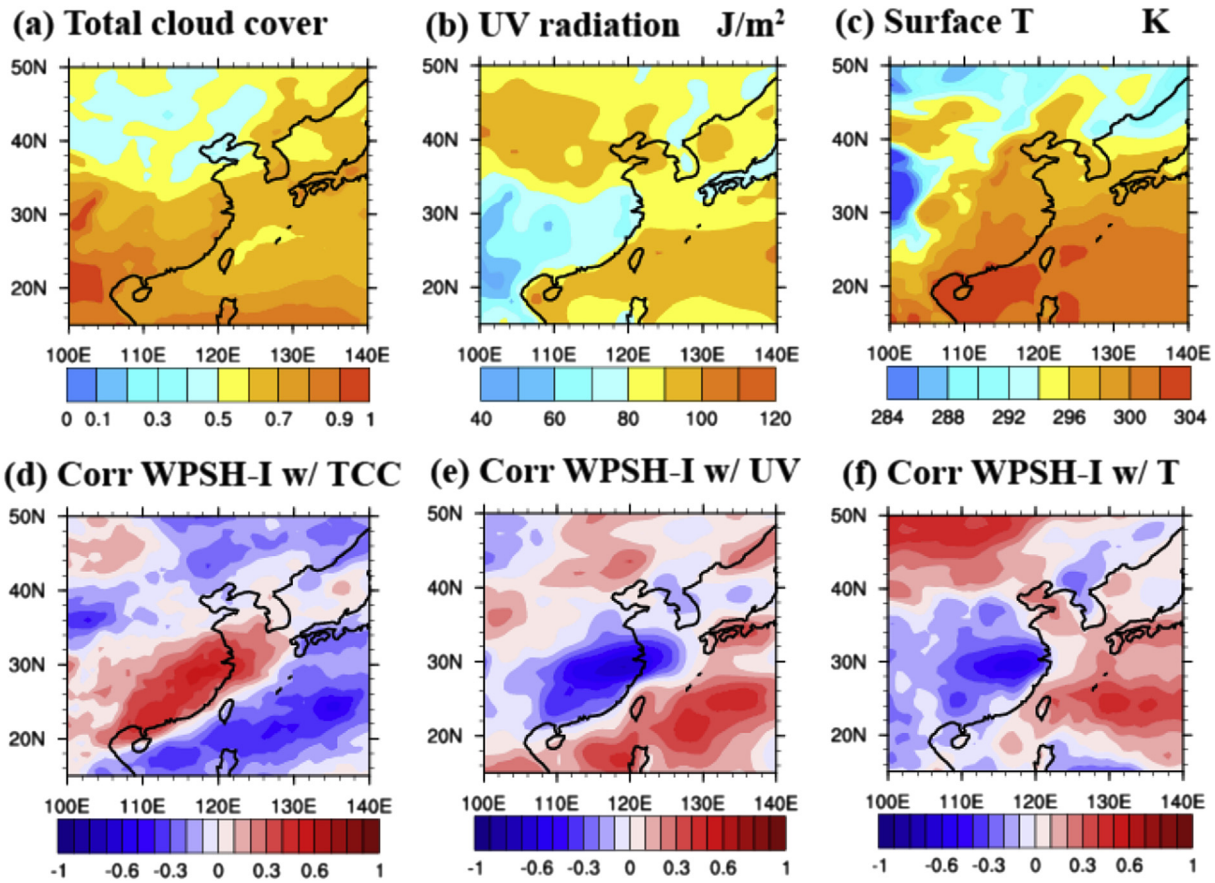

Fig. 6. (Upper panel) the summer mean fields of meteorological parameters and (lower panel) their correlations with the daily WPSH-I_anomalies: total cloud cover (a, d), downward UV radiation at the surface (b, e), and near-surface air temperature (c, f).

radiation. Since the photochemical formation of ozone is directly related with meteorological parameters, such as RH, radiation, and temperature, surface ozone concentrations become lower in SC and higher in NC when the WPSH intensity is strong, and vice versa.

6. Discussion and conclusions

In this study, we investigated the impacts of the WPSH variations on summertime surface ozone over eastern China on a daily scale using observations from recently established network of surface ozone monitors and meteorology reanalysis data during summer (June, July, August; JJA) 2014–2016 with a focus on 2014. A normalized WPSH intensity index (WPSH-I) was adopted here to characterize the daily variability of the WPSH. Correlation between WSPH-I and ozone is significantly negative in SC, and significantly positive in most parts of NC, with the average correlation coefficient of -0.36 ($p < 0.01$) and 0.20 ($p < 0.01$) respectively. The empirical orthogonal function (EOF) analysis revealed that the most distinctive pattern (EOF1) of daily MDA8 ozone variations during summer describes 25.2% of the total variance and displays a marked north-south contrast. Spatially, such a north-south contrast of the ozone EOF1 pattern is well correlated ($r = -0.86$, $p < 0.01$) with the distribution of WPSH-ozone correlations. In addition, the time series of ozone EOF1 pattern and WPSH-I anomalies show a temporally significant correlation, with r of -0.66 ($p < 0.01$). These tight associations between ozone EOF1 and WPSH-I suggest the dominant component of surface ozone daily variability in eastern China is linked with the variability of WPSH-I: a stronger WPSH intensity will lead to a decrease of surface ozone over SC but an increase over NC, and vice versa. The robustness of using WPSH-I as an indicator to establish the relationship of WPSH variability with surface ozone was verified by the comparison between the ERA and NCEP reanalysis datasets.

The linkage of surface ozone variability with WPSH-I is explained by the mechanism that the stronger WPSH intensity will bring stronger southwesterly winds to SC that transport moisture from the South China Sea to this region, thereby making such atmospheric conditions not conducive for ozone formation as higher RH, more cloudiness, less UV radiation, and lower temperature. On the contrary, as most of the rainfall due to the enhanced southwesterly transport of moisture occurs in SC, water vapor is largely depleted in the air masses transported towards NC. Therefore, the stronger WPSH intensity will bring drier atmospheric conditions less precipitation in NC, with lower RH, less cloudiness, and more UV radiation. Since the photochemical formation of ozone is directly related with meteorological parameters, such as RH, radiation, and temperature, surface ozone concentrations become lower in SC and higher in NC when the WPSH intensity is strong, and vice versa.

The relationship between WPSH-I and surface ozone is derived from observations during 2014–2016, a relatively short time period due to the lack of ozone monitoring network prior to 2014. The WPSHI-ozone relationship may require verification with longer-term observations when more data become available in the future. The relationship between WPSH intensity and surface ozone variations identified here provides a useful metric that may be used to forecast ozone concentrations and evaluate model performance in simulating meteorological drivers of ozone variability in east China.

Acknowledgement

This research was supported by the National Key Basic Research Program of China (2013CB956603 and 2014CB441302) and the CAS Strategic Priority Research Program (Grant No. XDA05100403).

Appendix A. Supplementary data

Supplementary data related to this article can be found at https://doi.org/10.1016/j.atmosenv.2017.09.024.

References

Bloomfield, P., Royle, J.A., Steinberg, L.J., Yang, Q., 1996. Accounting for meteorological effects in measuring urban ozone levels and trends. Atmos. Environ. 30, 3067–3077.
Camalier, L., Cox, W., Dolwick, P., 2007. The effects of meteorology on ozone in urban areas and their use in assessing ozone trends. Atmos. Environ. 41, 7127–7137.
Chen, T.C., Chen, J.M., Chen, T.C., Chen, J.M., 1993. The 10-20Day mode of the 1979 Indian monsoon: its relation with the time variation of monsoon rainfall. Mon. Weather. Rev. 121, 2465–2482.
Chen, Z.H., Cheng, S.Y., Li, J.B., Guo, X.R., Wang, W.H., Chen, D.S., 2008. Relationship between atmospheric pollution processes and synoptic pressure patterns in northern China. Atmos. Environ. 42, 6078–6087.
Davis, J.M., Speckman, P., 1999. A model for predicting maximum and 8 h average ozone in Houston. Atmos. Environ. 33, 2487–2500.
Ding, A., Wang, T., Fu, C., 2013. Transport characteristics and origins of carbon monoxide and ozone in Hong Kong, South China. J. Geophys. Res. 118, 9475–9488.
Ding, Y., 1994. The Summer Monsoon in East Asia. Springer, Netherlands.
Elminir, H.K., 2005. Dependence of urban air pollutants on meteorology. Sci. Total. Environ. 350, 225–237.
Fiore, A.M., Jacob, D.J., Mathur, R., Martin, R.V., 2003. Application of empirical orthogonal functions to evaluate ozone simulations with regional and global models. J. Geophys. Res. 108, 4431.
Gao, H., Jiang, W., Li, W., 2015. Changed relationships between the East Asian summer monsoon circulations and the summer rainfall in eastern China. J. Meteorol. Res. 28, 1075–1084.
He, J., Wang, Y., Hao, J., Shen, L., Wang, L., 2012. Variations of surface O3 in August at a rural site near Shanghai: influences from the West Pacific subtropical high and anthropogenic emissions. Environ. Sci. Pollut. Re.s Int. 19, 4016–4029.
Jacob, D.J., Winner, D.A., 2009. Effect of climate change on air quality. Atmos. Environ. 43, 51–63.
Kalnay, E., et al., 1996. The NCEP/NCAR 40-year reanalysis project B. Am. Meteorol. Soc. 77, 437–471.
Kinney, P.L., 2008. Climate change, air quality, and human health. Am. J. Prev. Med. 35, 459–467.
Lau, K.M., Peng, L., 2010. Origin of low frequency (intraseasonal) oscillations in the tropical atmosphere. Part III: monsoon dynamics. J. Atmos. Sci. 47, 1443–1462.
Leibensperger, E.M., Mickley, L.J., Jacob, D.J., 2008. Sensitivity of US air quality to mid-latitude cyclone frequency and implications of 1980–2006 climate change. Atmos. Chem. Phys. 8, 7075–7086.
Li, J., Wang, Z., Akimoto, H., Gao, C., Pochanart, P., Wang, X., 2007. Modeling study of ozone seasonal cycle in lower troposphere over east Asia. J. Geophys. Res. 112, 22–25.
Liu, H., Zhang, D.L., Wang, B., 2008. Daily to submonthly weather and climate characteristics of the summer 1998 extreme rainfall over the Yangtze River basin. J. Geophys. Res. 113, 1971–1976.
Lu, R., 2002. Indices of the summertime Western North Pacific subtropical high. Adv. Atmos. Sci. 19, 1004–1028.
Luo, C., John, J.C.S., Zhou, X., Lam, K.S., Wang, T., Chameides, W.L., 2000. A nonurban ozone air pollution episode over eastern China: observations and model simulations. J. Geophys. Res. 105, 1889–1908.
Pu, B., Dickinson, R.E., Fu, R., 2016. Dynamical connection between Great Plains low-level winds and variability of central Gulf States precipitation. J. Geophys. Res. 121, 3421–3434.
Shen, L., Mickley, L.J., Tai, A.P.K., 2015. Influence of synoptic patterns on surface ozone variability over the eastern United States from 1980 to 2012. Atmos. Chem. Phys. 15, 10925–10938.
Simmons, A.J., Uppala, S.M., Dee, D., Kobayashi, S., 2007. ERA-interim: New ECMWF Reanalysis Products from 1989 Onwards Ecmwf Newsl, vol 110, pp. 25–35.
Steiner, A.L., Davis, A.J., Sillman, S., Owen, R.C., Michalak, A.M., Fiore, A.M., 2010. Observed suppression of ozone formation at extremely high temperatures due to chemical and biophysical feedbacks. Proc. Natl. Acad. Sci. U. S. A. 107, 19685–19690.
Su, T., Xue, F., Zhang, H., 2014. Simulating the intraseasonal variation of the East Asian summer monsoon by IAP AGCM4.0. Adv. Atmos. Sci. 31, 570–580.
Sun, L., et al., 2016. Significant increase of summertime ozone at mount Tai in Central Eastern China. Atmos. Chem. Phys. 16, 10637–10650.
Tai, A.P.K., Mickley, L.J., Jacob, D.J., 2010. Correlations between fine particulate matter (PM2.5) and meteorological variables in the United States: implications for the sensitivity of PM2.5 to climate change. Atmos. Environ. 44, 3976–3984.
Tai, A.P.K., Mickley, L.J., Jacob, D.J., Leibensperger, E.M., Zhang, L., Fisher, J.A., Pye, H.O.T., 2012. Meteorological modes of variability for fine particulate matter (PM2.5) air quality in the United States: implications for PM2.5 sensitivity to climate change. Atmos. Chem. Phys. 12, 3131–3145.
Tao, S.Y., Xu, S.Y., 1962. Circulation characteristics in association with persistent summer drought and flood in the Yangtze-Huaihe River reaches. Acta Meteorol. Sin. 32, 1–10.
Wang, L., Guan, H., He, J., 2006. The position variation of the West Pacific subtropical high and its possible mechanism. J. Trop. Meteorol. 12, 113–120.
Wang, T., Wei, X.L., Ding, A.J., Poon, C.N., Lam, K.S., Li, Y.S., Chan, L.Y., Anson, M., 2009. Increasing surface ozone concentrations in the background atmosphere of Southern China, 1994–2007. Atmos. Chem. Phys. 9, 6217–6227.
Wang, Y., McElroy, M., Munger, J., Hao, J., Ma, H., Nielsen, C., Chen, Y., 2008. Variations of O3 and CO in summertime at a rural site near Beijing. Atmos. Chem. Phys. 8, 6335–6363.
Wang, Y., Zhang, Y., Hao, J., Luo, M., 2011. Seasonal and spatial variability of surface ozone over China: contributions from background and domestic pollution. Atmos. Chem. Phys. 11, 3511–3525.
Wang, Y., Jia, B., Wang, S.C., Estes, M., Shen, L., Xie, Y., 2016. Influence of the Bermuda High on interannual variability of summertime ozone in the Houston–Galveston–Brazoria region. Atmos. Chem. Phys. 16, 15265–15276.
Wilks, D.S., 2011. Statistical Methods in the Atmospheric Sciences. Academic press.
Worden, J., et al., 2009. Observed vertical distribution of tropospheric ozone during the Asian summertime monsoon. J. Geophys. Res. 114, 267–275.
Xu, X., Lin, W., Wang, T., Yan, P., Tang, J., Meng, Z., Wang, Y., 2008. Long-term trend of surface ozone at a regional background station in eastern China 1991–2006: enhanced variability. Atmos. Chem. Phys. 8, 2595–2607.
Yamaji, K., Ohara, T., Uno, I., Tanimoto, H., Kurokawa, J., Akimoto, H., 2006. Analysis of the seasonal variation of ozone in the boundary layer in East Asia using the Community Multi-scale Air Quality model: what controls surface ozone levels over Japan? Atmos. Environ. 40, 1856–1868.
Yang, Y., Liao, H., Li, J., 2014. Impacts of the East Asian summer monsoon on interannual variations of summertime surface-layer ozone concentrations over China. Atmos. Chem. Phys. 14, 6867–6879.
Zheng, J., Zhong, L., Wang, T., Louie, P.K., Li, Z., 2010. Ground-level ozone in the Pearl River Delta region: analysis of data from a recently established regional air quality monitoring network. Atmos. Environ. 44, 814–823.
Zhou, D., et al., 2013. Impacts of the East Asian monsoon on lower tropospheric ozone over coastal South China. Environ. Res. Lett. 8, 044011.
Zhou, T., et al., 2009. Why the Western Pacific subtropical high has extended westward since the late 1970s. J. Clim. 22, 2199–2215.
Zhu, J., Liang, X.Z., 2013. Impacts of the Bermuda high on regional climate and ozone over the United States. J. Clim. 26, 1018–1032.